



1    **Dynamics of Snow and Glacier Cover in the Upper Karnali Basin, Nepal: An Analysis of Its**

2    **Relationship with Climatic and Topographic Parameters**

3    Motilal Ghimire<sup>1</sup>, Dibas Shrestha<sup>2</sup>, Raju Chauhan<sup>3</sup>, Amrit Thapa<sup>4</sup>, Til Prasad Pangali Sharma<sup>5</sup>, Krishna

4    Prasad Sharma<sup>6</sup>, Sher Bahadur Gurung<sup>6</sup>, Sundar Devkota<sup>7</sup>, Prabin Bhandari<sup>8</sup>, Sikes Koirala<sup>7</sup>, Yanhong

5    Wu<sup>9</sup>, Niroj Timalina<sup>6</sup>, Jeevan Kutu<sup>6</sup>.

6    <sup>1</sup> Corresponding Author, Affiliation: Tribhuvan University, Central Department of Geography,

7    Kathmandu, Nepal. Email: [motighimire@gmail.com](mailto:motighimire@gmail.com)

8    <sup>2</sup>Tribhuvan University, Central Department of Hydrology and Meteorology, Nepal

9    <sup>3</sup>Tribhuvan University, Central Department of Environmental Science, Nepal

10    <sup>4</sup>University of Fairbanks, USA

11    <sup>5</sup>Tribhuvan University, Nepal Mountain Academy, Nepal

12    <sup>6</sup>Tribhuvan University, Central Department Geography, Nepal

13    <sup>7</sup>Government of Nepal, Department of Survey, Nepal

14    <sup>8</sup>George Mason University, USA

15    <sup>9</sup>Institute of Mountain Hazards and Environment, Chinese Academy of Sciences, China

16    **Abstract**

17    Snow and glacier cover in the Upper Karnali Basin (UKB) are crucial freshwater reservoirs that support

18    downstream ecosystems and human populations. This study uses remote sensing and GIS data from

19    various sources, MODIS-derived land surface temperature, and ERA5 reanalysis climate datasets to

20    analyze snow cover dynamics from 2002 to 2023/24. The results show a significant decrease in snow-

21    covered area (SCA), with an annual decline of about 3.99 km<sup>2</sup>. Seasonal variations indicate the most

22    significant reductions during the monsoon period (July-September), where rising temperatures accelerate



23 snowmelt. The analysis also establishes a strong negative correlation between snow cover and  
24 temperature ( $r = -0.59$  to  $-0.77$ ,  $p < 0.05$ ), with warming trends disproportionately affecting mid-to-high  
25 elevation zones (3000-5000 m a.s.l.). Glacier basins exhibit consistent retreat, with the mean glacier area  
26 declining from 119.046 hectares in 2000 to 100.472 hectares in 2023, highlighting the impact of climate  
27 change. Additionally, snowline analysis demonstrates an upward migration, with the 10th percentile  
28 snowline increasing at a rate of approximately 5.16 m/year, indicating progressive snow loss at lower  
29 elevations. These findings emphasize the vulnerability of UKB's cryosphere to climate change,  
30 necessitating adaptive water resource management strategies. This will help mitigate impacts on  
31 hydrology, agriculture, and regional water security.

32 **Keywords:** Snow and glacier, Karnali, Himalayas, Remote sensing, Climate Change, Elevation-  
33 depended-warming, Snowline

34



## 35        **1. Introduction**

36        Snow and glaciers in the mountains function as freshwater towers. Meltwater from mountain snow and  
37        glaciers releases water, providing a consistent supply for rivers and downstream ecosystems (Immerzeel  
38        et al., 2020; Wester et al., 2019; Pritchard, 2019). Snow and glaciers in the Himalayas play a crucial role  
39        and present opportunities for economic development and an improved quality of life for the local  
40        population(Pritchard, 2019). A decline in snow and glaciers will negatively affect water availability in the  
41        region (Krishnan et al., 2019). The alpine and downstream communities of Nepal, India, and China rely  
42        on snow and glacial meltwater for drinking, agriculture, livestock, electricity generation, and other needs  
43        (Bolch, 2007; Bookhagen and Burbank, 2010).

44        Furthermore, snow and glacial ice regulate regional and global climates by reflecting solar radiation,  
45        thereby, contributing to the Earth's energy balance and influencing local weather patterns (Xu et al.,  
46        2009). Seasonal meltwater from glaciers and snow impacts ecosystems that provide habitats for numerous  
47        animal and plant species in the mountains. These organisms have adapted to the water availability from  
48        the mountain cryosphere. As a result, changes in snow cover and glaciers can disrupt entire ecosystems  
49        (Wester et al., 2019). On both local and regional scales, variations in the amount of snow and ice can  
50        contribute to changes in sea level, affecting coastal areas (Forster et al., 2021; Mimura, 2013; NOAA,  
51        2013).

52        Snow-covered peaks and glaciers attract adventure tourism, while the glaciated landscape offers  
53        opportunities for nature-based aesthetic, recreational, and religious tourism (Anup, 2017; Nyaupane and  
54        Chhetri, 2009). Snow and glaciers are sensitive to climate change; shifts in their size and volume provide  
55        insights into broader climate trends and serve as visible indicators of environmental change.

56        There is growing concern that global warming is altering the cryosphere, with significant implications for  
57        human welfare and ecosystems (Elsasser and Bärki, 2002). Understanding how changes in snow and  
58        glaciers will impact future hydrology, water availability, and cryospheric hazards necessitates systematic,



59 long-term assessment and monitoring. Historically, large-scale snow cover data were limited, especially  
60 in remote and less populated regions. However, advancements in satellite remote sensing since the 1970s  
61 have made snow cover mapping more accessible and routine. Accurate monitoring of snow cover is  
62 essential for managing water resources, promoting economic development, and mitigating risks  
63 associated with cryospheric disasters (Muhammad and Thapa, 2020). This is particularly critical in  
64 regions where snowmelt is a primary source of river discharge, such as the Himalayan river basins.  
65 Studies have revealed a significant reduction in snow-covered areas and accelerated glacial melting in the  
66 region over recent decades (Bajracharya et al., 2014; Bolch et al., 2012; Gurung et al., 2017; Andreas  
67 Kääb et al., 2012; Krishnan et al., 2019; Kulkarni et al., 2021; Mishra et al., 2014; Mool et al., 2001; Arun  
68 B Shrestha and Aryal, 2011). These studies emphasize the critical role of cryospheric changes in shaping  
69 the region's hydrology, affecting the magnitude and seasonality of drinking water supply, irrigation, and  
70 the country's energy production from hydropower. Integrating remote sensing data, ground-based  
71 observations, and climate models has been effective in assessing and predicting changes in snow and ice  
72 dynamics

73 A vast body of literature exists on Nepali Himalayan glaciers, glacier lakes, and glacier lake outburst  
74 floods (GLOFs), offering insights into cryosphere dynamics and climate variability since the  
75 1960s (Bajracharya et al., 2008; Hall et al., 2002; A Kääb et al., 2005; Maheswor Shrestha et al., 2012;  
76 Zemp, 2006). However, most studies focus on the central and eastern Himalayas of Nepal, leaving the  
77 mid-western and far-western regions underexplored due to their remoteness, limited accessibility, and  
78 lack of attention. While global and regional glacier inventories cover these areas in-depth, more focused  
79 studies of snow and glacier cover change using high spatial resolution detailed studies  $\leq 30$  m, Elevation  
80 Dependent Warming (EDW) and snow cover trend are limited (Bajracharya et al., 2014; Bishop et al.,  
81 2004; Heid and Kääb, 2012). Integrating glaciers, glacier basins, and snow cover while linking them to  
82 climate change is also under-examined.



83 Bridging this spatial knowledge gap through focused research on cryosphere dynamics in these regions is  
84 crucial. It will enhance the understanding of long-term changes and provide evidence-based data to  
85 inform policies on ecology, hazards, water availability, and food security, benefiting both alpine and  
86 downstream populations.

87 The Karnali Basin is the largest river basin in Nepal, home to ~2.5 million people  
88 ([www.censusnepal.cbs.gov.np](http://www.censusnepal.cbs.gov.np)). The Karnali River system drains an area of 40,780 km<sup>2</sup> over the  
89 Chisapani gauge station. The snow and glacier-fed waters in the basin provide irrigation for millions  
90 living within and across the Indo-Nepal border, especially during the dry season. Additionally, snow and  
91 glaciers supply moisture and water for agro-pastoralism, the primary livelihood of local communities in  
92 alpine regions. Despite their significant freshwater sources, high ecological value, and potential for  
93 hydropower and tourism-based prosperity, snow and glaciated areas in the Karnali Basin have remained a  
94 frontier for cryosphere studies.

95 While extensive literature exists on snow, glaciers, and glacial lakes in the central and eastern Himalayas  
96 of Nepal, as well as in the Indian Himalayas and adjacent Tibetan Plateau, the findings of these studies  
97 cannot be reliably applied to the Karnali Basin due to differing climatic regimes and trends in various  
98 geographical settings. Understanding the impacts of cryosphere change on water resources necessitates  
99 studies specific to the status and dynamics of the cryosphere in the Karnali Basin. Additionally,  
100 integrating MODIS data with high temporal but lower spatial resolution and Landsat series data with low  
101 temporal but higher spatial resolution will enhance our understanding of snow and glacier changes,  
102 revealing trends in snow cover and their connections to topography, glacier basins, and climate  
103 fluctuations.

## 104 **2. Study area**

105 The Upper Karnali Basin, located between 28.64-30.68° N and 80.64-83.54° E, covers 22,577 km<sup>2</sup> and  
106 includes sub basins drained by the Humla Karnali, Mugu Karnali, Kawari, and Tila Nadi rivers (Ghimire



et al., 2024) (Figure 1). The elevation ranges from 340 m to 7030 m, with an alpine zone above 4000 m consisting of snow, glaciers, and bare rocks. The climate varies from Polar Tundra in the glacier region to subtropical, temperate, and cold climates below 4000 m, with mean annual temperatures ranging from 27°C to <-12°C and precipitation from 1000 to 800 mm annually.

The Upper Karnali Basin features a diverse landscape of snow-covered glaciers, valleys, permafrost, alpine meadows, and forests, along with a rich variety of flora and fauna. It is a cultural blend of Khas and Tibetan traditions and is a growing tourist destination, including a stop on the Kailash Mansarovar pilgrimage route. The basin has a population of approximately 816,941 people with a density of 36.2 persons/km<sup>2</sup>, residing in 4,395 settlements primarily below 4000 m. The Human Development Index in the area is below the national average at 0.49.

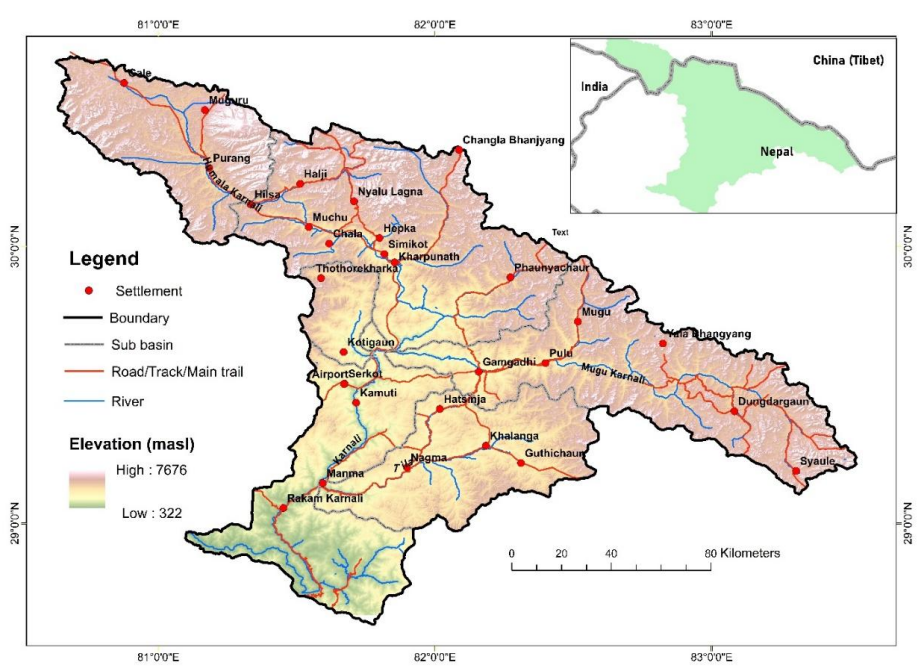


**Figure 1. Location of the Upper Karnali Basin.**



120

### 121       **3. Data Sources and Method**

122       To achieve its objectives, the study employed remote sensing technology alongside various data sources.

123       It employed coarse-to-moderate-resolution optical and thermal satellite imagery from MODIS Aqua and

124       Terra, Landsat TM5, ETM 7, and OLI 8, accessed through the Google Earth Engine platform(Gorelick et

125       al., 2017; Hall et al., 2002). This imagery was used to gather time series data on snow and ice cover and

126       land surface temperature.

127       To generate a snow cover map using Google Earth Engine (GEE) and Landsat data, we began by

128       accessing the GEE Code Editor. We loaded the relevant Landsat Image Collection (Landsat 5, 7, or 8) and

129       filtered the data by specifying the time range, area of interest (Upper Karnali Basin), and acceptable cloud

130       cover. Imageries were preprocessed by masking clouds using the Quality Assessment (QA) bands

131       (pixel\_qa for Landsat 5/7 or QA\_PIXEL for Landsat 8). Then Normalized Difference Snow Index (NDSI)

132       was then calculated using Green and Short-wave infrared bands (Gorelick et al., 2017; Hall et al., 2002).

133       Then, a threshold  $NDSI > 0.4$  was applied to isolate snow cover pixels from others. Finally, we exported

134       the snow cover map as a GeoTIFF file for further overlay analysis with sun-basin and microglacier

135       basins.

136       MODIS snow cover data (MOD10A1) was processed using Google Earth Engine (GEE)(Hall et al., 2002)

137       for the Upper Karnali region. The cloud-masked snow cover data was classified into four seasonal

138       composites: January–March, April–June, July–September, and October–December. Elevation bands were

139       defined based on the SRTM DEM and categorized as below 3000 m, 3000–4000 m, 4000–5000 m, and

140       above 5000 m. Zonal statistics were applied to extract the frequency of snow cover for each elevation

141       band and subbasin. The snow-covered area was calculated using a threshold-based binary mask. The

142       results were aggregated into a structured dataset, revealing seasonal snow distribution and variations

143       across elevation zones and watersheds, thus facilitating hydrological analysis.



144 The land surface temperature (LST) was also downloaded from the Application for Extracting and  
145 Exploring Analysis Ready Sample (AppEEARS) platform. AppEEARS is a NASA-supported platform  
146 developed to easily access, subset into specified areas, and analyze climate and environmental data.  
147 Temperature and precipitation data, including maximum and minimum values, were procured from the  
148 Government of Nepal's Department of Hydrology and Meteorology and open-access platforms such as the  
149 ERA5 Reanalysis.

150 The time series glacier data compiled by Ghimire et al. (2024) (submitted) was included in the study. The  
151 same lead author of this manuscript was responsible for the research paper. In summary, glacier polygons  
152 for the years 2000, 2010, and 2023 were mapped using high-resolution images (from Google Earth, Bing  
153 Maps, and Rapid Eye) from 2000 and 2023 to maintain temporal consistency. Snow and glaciers were  
154 identified based on their bright spectral features, smooth textures, and shadows on nearby terrain. Landsat  
155 composites (both true and false color) and band ratios like NDSI improved the visibility of snow and ice,  
156 while altitude and topographic data derived from DEM highlighted potential glacier regions. Outlines  
157 from the Randolph Glacier Inventory (RGI)(Pfeffer et al., 2014) and ICIMOD (Bajracharya et al., 2014)  
158 were used as reference points, while ground-truth observations and additional datasets helped validate the  
159 findings. This comprehensive approach ensured precise delineation.

### 160 **3.1. Delineation of the glacier basin**

161 The boundaries of glacier basins were defined to evaluate the snow cover fraction in glacier-drained  
162 areas. Glacier basins are regions that encompass both central and sub-glaciers fed by moving ice and  
163 snow. Their boundaries are marked by the main glacier's terminus. The process involved multiple steps to  
164 ensure precision.

165 Initially, the Glacier Inventory map referenced earlier served as a fundamental resource. High-resolution  
166 imagery and ESRI's topographic maps in ArcGIS 10+ supplied intricate spatial data. A 12.5 m DEM was  
167 utilized to extract drainage networks, produce contour lines, and generate hillshade maps, which





168 improved the visualization of the divides between glacier basins. These components were vital for  
169 pinpointing the glacier terminus and outlining glacier head basins. This holistic approach, merging  
170 topographic analysis, remote sensing, and geospatial techniques, facilitated the precise delineation of  
171 glacier basins for comprehensive evaluations of snow cover fraction.

### 172 **3.2. Limitations**

173 This study encountered limitations due to significant cloud cover, making cloud-free conditions  
174 infrequent for Landsat during the pre-monsoon and monsoon periods. Consequently, snow cover data  
175 from Landsat was accessible only for the months of January through March and October through  
176 December in the Upper Karnali sub-basins. Nonetheless, all four seasons were examined for micro glacier  
177 basins where data was dependable. To address this limitation, MODIS (MOD10A1) data was employed.  
178 This method also enabled a comparison between the data obtained from Landsat's higher spatial  
179 resolution (30 m) but lower temporal resolution (16 days) and MODIS's daily high temporal resolution  
180 with lower spatial resolution (500 m).

## 181 **4. Result**

### 182 **4.1. Snow or ice cover trend and variability: Annual and seasonal**

183 The total snow cover across the Upper Karnali Basin (22,546 km<sup>2</sup>) from 2002–2024 averages 872 km<sup>2</sup>,  
184 with a standard deviation of 147 km<sup>2</sup>, indicating moderate variability (Table 1 and Figure 2 ). The  
185 minimum recorded snow cover is 424.25 km<sup>2</sup>; about 25% of the recorded snow cover observations are at  
186 or below 640.32 km<sup>2</sup>. The average snowfall from January–March is (1528 ±333 km<sup>2</sup>), followed by April–  
187 June (881 ± 212 km<sup>2</sup>) and October–December (862±373 km<sup>2</sup>), respectively. July to September witnessed  
188 the lowest snow cover area, i.e., 212 ±38.3 km<sup>2</sup>.

189 Snow cover data highlights significant year-to-year changes in every quarterly season with varying  
190 directions and magnitude of trends, evidenced by correlation, the Kendall tau test, and Sen's slope. The  
191 annual average SCA shows, although not significant, a decreasing trend (p = 0.535), with Sen's Slope



estimating a loss of ~3.99 km<sup>2</sup>/year, which indicates a gradual decline in snowpack over two decades. Seasonally, the July–September period exhibits the statistically significant steepest drop in snow cover (Sen's Slope = -2.87,  $p = 0.00$ ). This period is snow ablation, where the summer monsoon brings warmer temperatures. In mid-latitude regions, the precipitation occurs more as rain than snow, resulting in accelerated snowmelt. While January–March shows a decline (Sen's slope = -8.63 km/year), it lacks statistical significance ( $p = 0.523$ ), suggesting year-to-year winter variability in snowfall or early melt. Similarly, no significant trends were detected in April–June. Interannual variability is evident with peaks and lows of snow and ice coverage (Figure 2). Episodic snow coverage in 2015, 2020, and 2022 (January–March), 2015 and 2019 (April–June), 2009, and 2021 (October–December), high episodic heavy snowfall years. However, these anomalies do not counterbalance long-term declines. Compared to seasons, annual snow coverage's inter-annual variability is relatively low, i.e., with a 16% coefficient of variation (CoV)–ratio of the standard deviation to the mean.

**Table 1. Snow cover descriptors and changes by seasons**

Descriptors	January– March	April– June	July– September	October– December	Annual average
Mean	1528	881	217	862	872
Median	1569	858	210	739	886
Std. dev.	333	212	38.3	373	147
Minimum	1025	503	169	340	514
Maximum	2167	1358	298	1737	1055
Skewness	0.211	0.47	0.937	0.509	-0.867
25 th Percentile	1270	751	191	538	777
50 th Percentile	1569	858	210	739	886
75 th Percentile	1689	1025	229	1126	991
Correlation	-0.087	-0.069	<b>-0.610</b>	-0.251	-0.274
Kendall's Tau	-0.091	0.013	<b>-0.541</b>	-0.134	-0.100
P value	-0.523	0.95	0.00	0.398	0.535
Sen's slope	-8.63	-3.14	-2.87	-13.21	-3.99

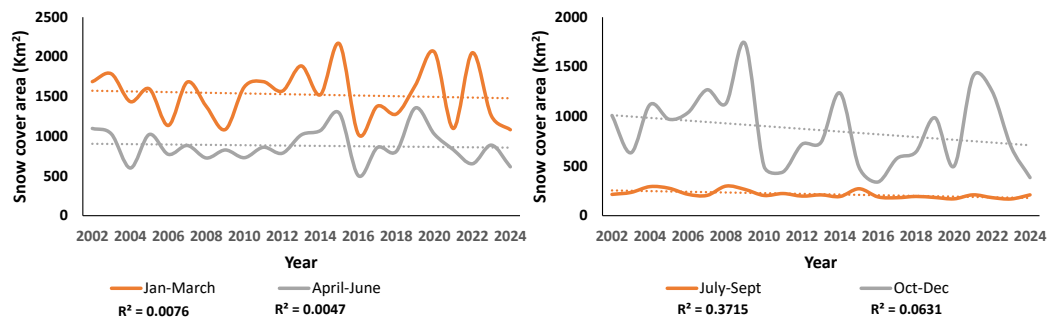
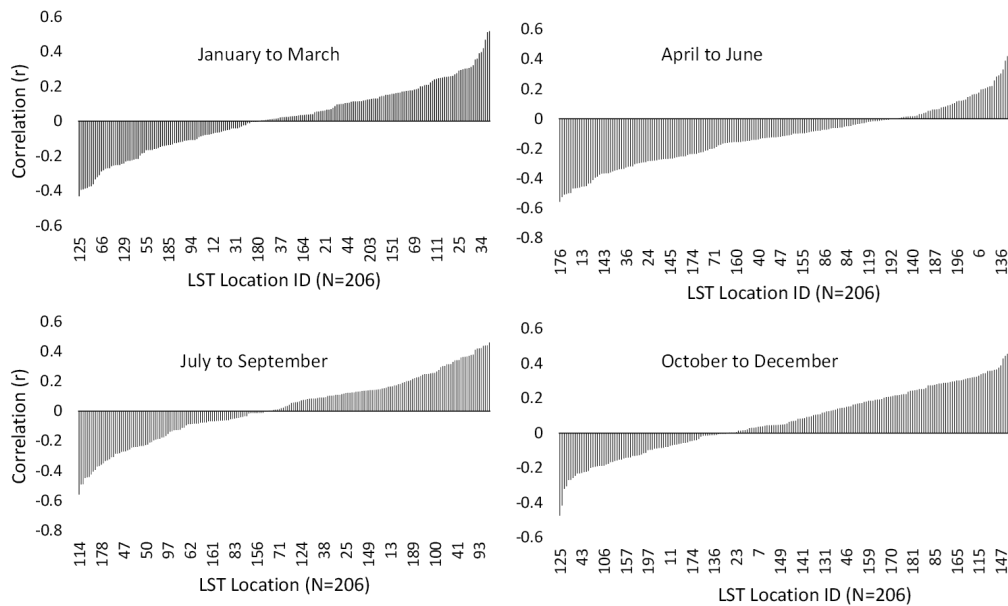


**Figure 2. Snow cover trend in Upper Karnali Basin in different seasons.**

#### **4.2. The relation among snow cover, temperature, and precipitation**

There is some spatial variation in the temperature trend, although negative correlations dominate most of the 204 sampled locations in all seasons except for the months April–June (Figure 3). The average rainfall across the 204 locations also shows a declining trend in all seasons except for June–July (Figure 4). The effect of precipitation on snowfall may influence the predominance of negative temperature correlations over time.

We generalized temperature data derived from MODIS Terra (MYD11A1) and Aqua (MOD11A2) Land Surface Temperature (LST), processed through AppEEARS, along with precipitation data sourced from the ERA5-Land reanalysis by ECMWF (Hersbach et al., 2020), collected from 204 locations across four different periods to examine the relationships between snow cover, temperature, and precipitation (Figure 5). The snow-covered area shows a strong to moderate negative correlation ( $r = -0.59$ – $-0.77$ ,  $p < 0.05$ ) with temperature across all seasons. Conversely, precipitation has a positive correlation ( $r = 0.55$ – $0.59$ ,  $p < 0.05$ ) with snow cover for January–March and October–December, while during the remaining months, it shows a moderate negative correlation with negative trends. Precipitation and temperature display a negative correlation for January to March–October to December; during the summer months (April–September), these climatic variables also exhibit a positive correlation.



225

226 **Figure 3. The correlation ( $r < -0.40$  or  $< 0.40$ ,  $P < 0.05$ ) illustrates the temperature trend directions at**  
227 **various sites between 2000 and 2024 (Source: MODIS Terra and Aqua MOD11A2, MYD11A1,**  
228 **AppEEARS).**

229

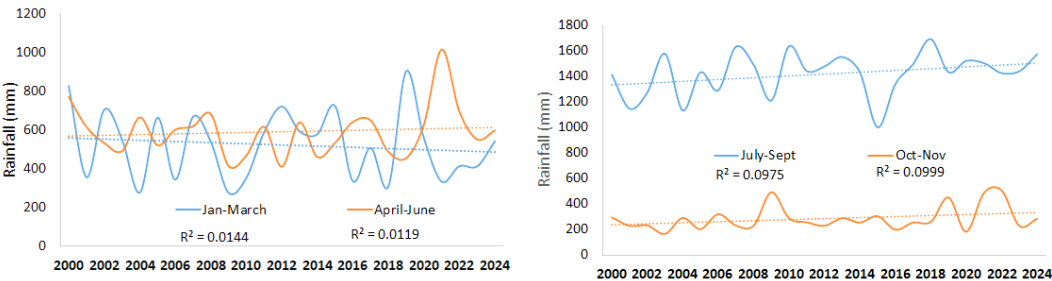


**Figure 4. Yearly rainfall trends across various periods. Precipitation data was collected from the ERA5-Land reanalysis by ECMWF (Hersbach et al., 2020) from 204 locations across four different periods.**

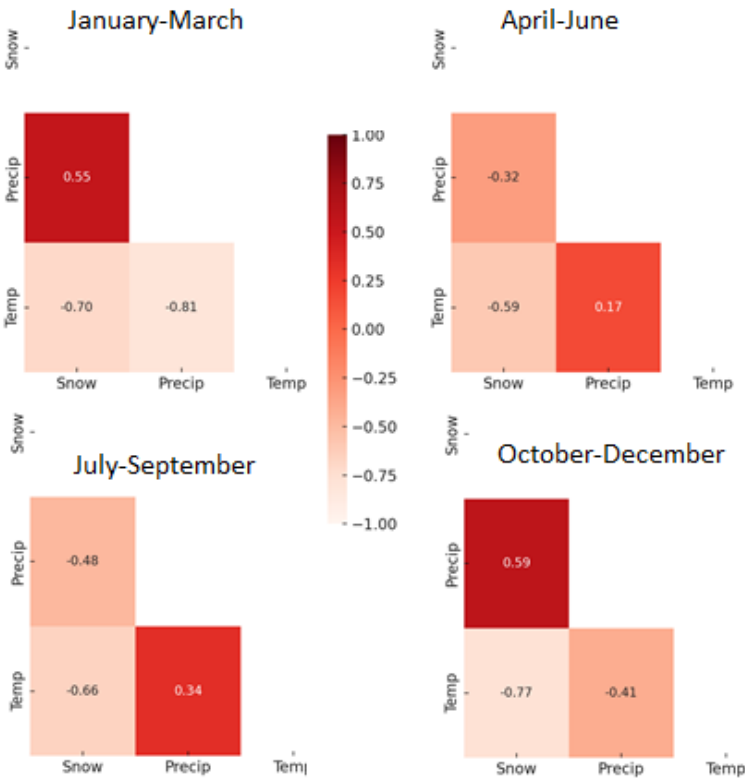


**Figure 5. Relationship among snow, temperature, and precipitation**



#### 237      **4.3.Snow cover changes in sub-basins using Landsat series data**

238      Due to the unavailability of Landsat-derived reliable snow and ice data in pre-monsoon and monsoon due  
239      to significant cloud coverage (as mentioned in section), only two seasons, January–March and October–  
240      November were considered. These seasons correspond to snowfall as precipitation that contributes to  
241      snow accumulation.

242      Examining snow cover patterns in the Upper Karnali Basin (UKB) sub-basins for two seasons January–  
243      February and October–December reveals notable seasonal and spatial differences (Table 2). During  
244      January-February, Humla Karnali has the largest average snow cover at 3,336 km<sup>2</sup>, followed by Mugu  
245      Karnali at 1,864 km<sup>2</sup> and China Karnali at 1,478 km<sup>2</sup>, while areas downstream like Tila and Kawari have  
246      very little coverage (less than 350 km<sup>2</sup>). There is significant variability in snow cover, particularly in Tila  
247      and Downstream Karnali, which has a coefficient of variation above 50%, indicating inconsistent  
248      snowfall from year to year from January–March, although associated with a significant negative  
249      correlation, i.e.,  $\geq -0.37$  ( $p < 0.1$ ) (Figure 6). The skewness of the temporal distribution is moderately  
250      negative, which does not affect the correlation, which is negative for all the basins, indicating a declining  
251      trend.

252      Conversely, the October-December season has lower average snow cover (823 km<sup>2</sup>) with strong  
253      fluctuations (e.g., 1570–227 km<sup>2</sup> and CoV=55%). Strong variability (CoV) is observed for all basins,  
254      particularly China Karnali, Tila and Downstream Karnali, the variability is strongest. The skewness is  
255      moderate, except Downstream Karnali and correlation values are reliable and indicate a declining trend.  
256      However, Downstream Karnali, in spite of high variability, indicates a statistically significant negative r  
257      value, i.e.,  $-0.47$  ( $p < 0.05$ ) (Figure 6).

258

259

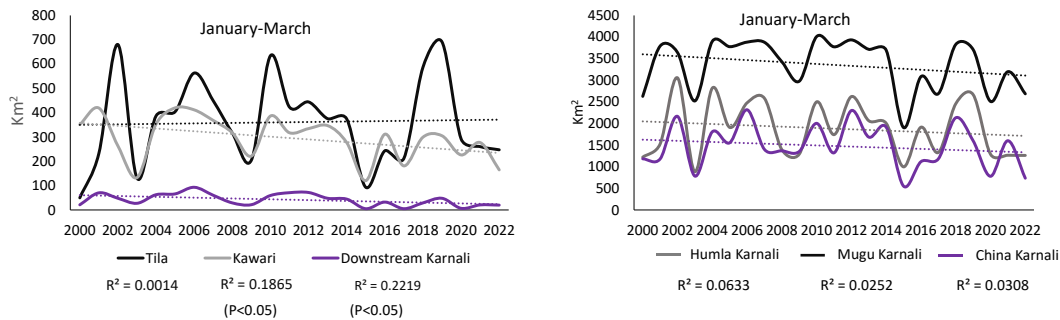


Table 2. Descriptive statistics of snow cover across sub-basins for two seasons (January-March and October-December) and the time series correlation from 2002 to 2024.

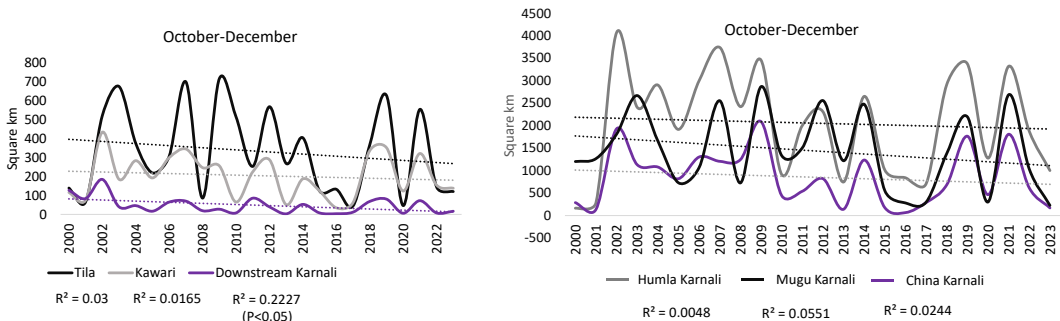
Descriptor	January - March						October-December							
	China Karnali	Humla Karnali	Mugu Karnali	Tila	Kaweri	Down stream	Seasonal average	China Karnali	Humla Karnali	Mugu Karnali	Tila	Kaweri	Down stream	Seasonal average
Mean	1478	3336	1864	351	294	41.9	1227	854	2057	1442	332	204	48.1	823
Median	1420	3667	1827	346	308	39	1239	754	2159	1301	288	190	40.2	781
Standard deviation	501	597	645	184	86.2	24	311	622	1163	862	227	112	44.7	457
Coefficient of variation (CoV in %)	33.90	17.90	34.60	52.42	29.32	57.28	25.35	72.83	56.54	59.78	68.37	54.90	92.93	55.53
Minimum	552	1904	887	50.1	121	5.74	612	67.2	166	226	44.3	35.2	3.28	227
Maximum	2317	4009	3056	691	420	93.5	1642	2092	4074	2868	716	434	185	1570
Skewness	-0.707	-0.488	-1.29	-0.69	-0.469	-0.763	-1.1	0.533	-0.016	0.231	0.347	0.204	1.43	0.202
Correlation (r<-0.44 and r>0.44, p<0.05)	-0.16	-0.18	-0.10	0.12	-0.37	-0.41	-0.14	-0.16	-0.07	-0.23	-0.17	-0.13	-0.47	-0.17



261



262



263

264 **Figure 6. The snow cover trend in the Upper Karnali Basin varies across different sub-basins from**  
265 **January–March and from October–December.**

266 **4.4. Snow cover dynamics across elevation zones**

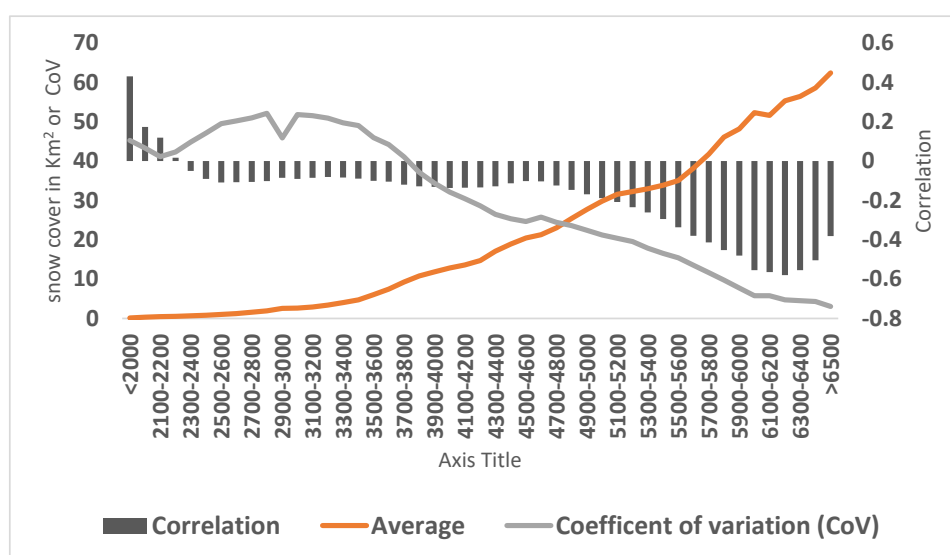
267 The dynamics of snow cover across elevation zones, categorized in 100-meter intervals from  $\leq 2000$  m to  
268  $\geq 6500$  m, reveal remarkable elevation-dependent patterns in correlation and variability (Figure 4). Snow  
269 cover in lower elevation zones shows a weak positive correlation (0.12-0.43), suggesting a marginal  
270 increase. However, pronounced interannual variability (CoV ~ 41-43%) is likely driven by fluctuating  
271 temperature and precipitation regimes (Pendergrass, 2020).





272 Above 2300 m a.s.l., correlations shift to weak negative correlations (up to 5000 m a.s.l.,  $r = 0.05$ - $0.17$ )  
 273 and moderate correlation upto 4800 m, then after, reaching peak negativity at 6100-6200 masl ( $r = -0.56$ ),  
 274 indicating a significant decline in snow cover over two decades (Figure 7). This trend aligns with the  
 275 impacts of global warming, where rising temperatures disproportionately affect higher elevations,  
 276 accelerating snowmelt and reducing accumulation (Shaoting Ren et al., 2023; Shen et al., 2021; Naegeli  
 277 et al., 2019). The mean snow cover increases with elevation, showing a marked rise from 3300 to 6500 m  
 278 a.s.l. or above, except between 5000-5000 m a.s.l.. which exhibits a gradual rise of snow cover.

279 Above this point, the mean snow cover area rises sharply, coinciding with glaciers and permanent snow  
 280 zones. In contrast, the CoV increases with elevation up to 3100 m a.s.l.. and then trends sharply  
 281 downward from 3100 m a.s.l. to 6500 m a.s.l. and beyond. This pattern indicates a decline in interannual  
 282 variability alongside increased negative correlations. The low inter-variability implies a reliable declining  
 283 trend in snow cover elevation.

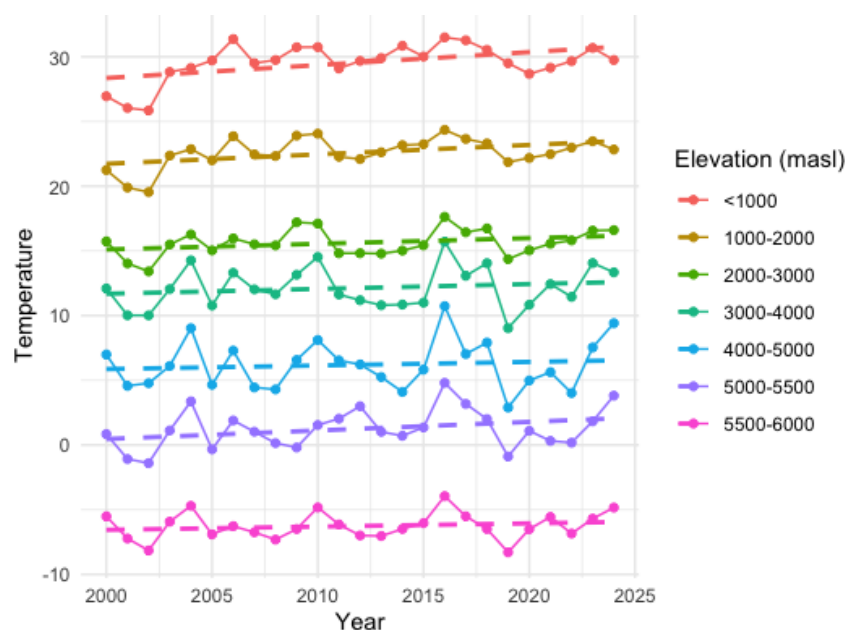


285 **Figure 7. The average, coefficient of variation, and correlation of snow cover area across various**  
 286 **elevation bands.**



287 To examine the relation between temperature and snow cover, the elevation bands were regrouped into  
 288 seven broader bands: below 2000, 2000–3000, 3000–4000, 4000–5000, 5500–6000, and above m a.s.l...  
 289 Figure 5 shows that the temperature has risen in all elevations. The temperature trend from 2002 to 2024  
 290 across elevation bands in the Upper Karnali Basin, as evidenced by Sen's slope (Figure 8, Table 3), shows  
 291 a general increase, with the highest rate of change observed at lower elevations (<1000 m:  
 292 0.0765°C/year). Mid-elevations (1000-2000m: 0.0576°C/year) and high elevations (5000-5500m:  
 293 0.0643°C/year) also exhibit warming. However, statistical significance (P-value) weakens at higher  
 294 elevations. This warming accelerates glacier retreat, reducing snow cover and impacting hydrology,  
 295 leading to declining glacier-fed water supply and altering river flow patterns in the Upper Karnali Basin.

296



297

298 **Figure 8. Temperature trend between 2002 and 2024 for different elevation bands**

299

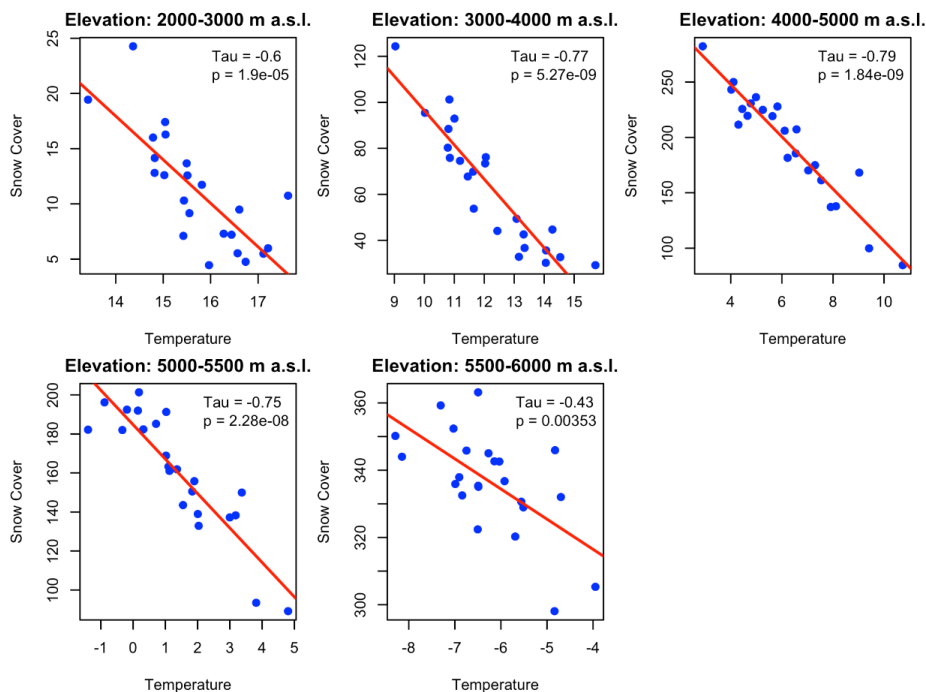


300

301 **Table 3. Rate of temperature change in different elevation between 2000-2024)**

Elevation bands (m a.s.l.)	Sen's slope	P Value
<1000	0.0765	0.052
1000-2000	0.0576	0.058
2000-3000	0.0390	0.168
3000-4000	0.0410	0.528
4000-5000	0.0198	0.833
5000-5500	0.0643	0.154
5500-6000	0.0287	0.414

302 Figure 9 shows a strong negative correlation between land surface temperature and snow cover across  
 303 elevation bands in the Upper Karnali Basin. Tau values range from -0.43 to -0.79, indicating that as  
 304 temperature rises, snow cover declines significantly. The correlation is strongest between 3000-5000 m  
 305 a.s.l.. (Tau = -0.77, -0.79) and 5000-5500 m a.s.l. (Tau = -0.75), with all p-values <0.01, confirming  
 306 statistical significance. Even at 5500-6000 m a.s.l. (Tau = -0.43, p = 0.00353), snow cover continues to  
 307 decline. The impact is most severe at mid-to-high elevations, where warming accelerates snowmelt and  
 308 glacier retreat. This trend threatens water availability in the Upper Karnali Basin, affecting river flows,  
 309 agriculture, and hydropower. The findings highlight the vulnerability of high-altitude regions to climate  
 310 change, with rising temperatures disrupting the region's hydrological balance. Continuous warming will  
 311 likely exacerbate glacial retreat, reducing freshwater storage and increasing water-related risks for  
 312 downstream communities.



313

314 **Figure 9. Relationship between snow cover and temperature (Celsius) across elevation zones in the**  
315 **Upper Karnali Basin (2002–2024).**

316 **4.5. Snow cover the trend in Glacier Basins (Landsat data).**

317 We examined snow cover trends in glacier basins containing at least a glacier in 2000, greater than 10  
318 hectares (# 735), which are crucial for assessing glacial status, water security, and climate change impacts  
319 (Table 4). The minimum altitude of the glacier basin where all tributary glaciers meet was considered an  
320 outlet of glacier basins. The rationale behind selecting glacier basins as the unit analyzing the snow cover  
321 trend is that glacier basins are the primary source of glacier mass accumulations. In these basins, snowfall  
322 restocks ice lost to melting, contributing to glacier stability and sustenance. Reduced snow cover in the  
323 glacier basins accelerates negative mass balance, a state where melting exceeds accumulation, leading to  
324 glacier retreat. These glacier basins are at a minimum altitude above 4000 m a.s.l. with an average of  
325 ~5100 m a.s.l.. Twenty-five and 75 % lie below 4800 and 5330 m a.s.l., respectively. Besides other



meteorological parameters, current temperature trends and albedo patterns play a critical role in glacier mass balance (Ye and Tian, 2022; Dowson et al., 2020). Higher temperatures directly increase the snow melting rate, and a decrease in reflectivity of solar radiation leads to more solar radiation being absorbed by the glacier surface, leading to accelerated melting and a negative mass balance (Shaoting Ren et al., 2023). Declining permanent snow cover in the glacier basin disrupts the glacier mass balance, affects the glacier persistence, alters the water availability, and accentuates the climate-driven environmental changes.

The data reveals a significant decline in glacier area across 734 glacier basins between 2000 and 2023 (Table 4). The mean glacier area decreased from 119.046 ha in 2000 to 100.472 ha in 2023, reflecting an average loss of 18.574 ha per basin. The total glacier area shrank by 13,633.163 ha, indicating widespread glacier retreat. The percent of glacier area to total basin area declined from 53.23% in 2000 to 44.93% in 2023, indicating a relative reduction in glacier coverage. Statistical tests show high skewness ( $>3.9$ ), suggesting that a few large glaciers dominate the dataset. The Shapiro-Wilk test ( $p < .001$ ) confirms a non-normal distribution.

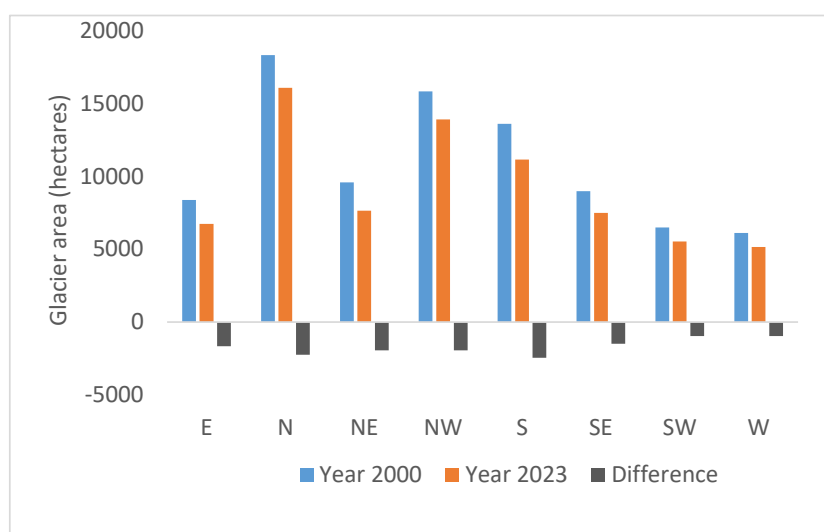
**Table 4. Change in glacier area between 2000 and 2023.**

Glacier basin count (N=735)	Glacier basin Area (hectares)	Glacier area (hectares)		Difference in glacier area (hectares)
		2000	2023	
Median	101.4	52.8	39.7	-10.0
Mean	223.6	119.0	100.5	-18.6
Std. Dev	368.1	187.1	169.9	27.2
Skewness	4.6	4.0	4.0	-4.0
Sum	164140.9	87379.9	73746.8	-13633.2

The glacier area has declined across all basin directions from 2000 to 2023, with the basins oriented toward North (N), Northwest (NW), and Northeast (NE) experiencing the largest losses, totaling -6,126.9 hectares (Figure 10). Eastern (E), Northeast (NE), and Southwestern (SW) glaciers also show significant reductions, although less severe.



345 The southern (S) and southeastern (SE) basins experienced significant shrinkage, indicating a widespread  
346 retreat. The negative differences across all directions confirm a consistent loss in glacier coverage, likely  
347 due to rising temperatures and decreased snowfall. These trends emphasize the ongoing effects of climate  
348 change on glacier-fed regions.



349

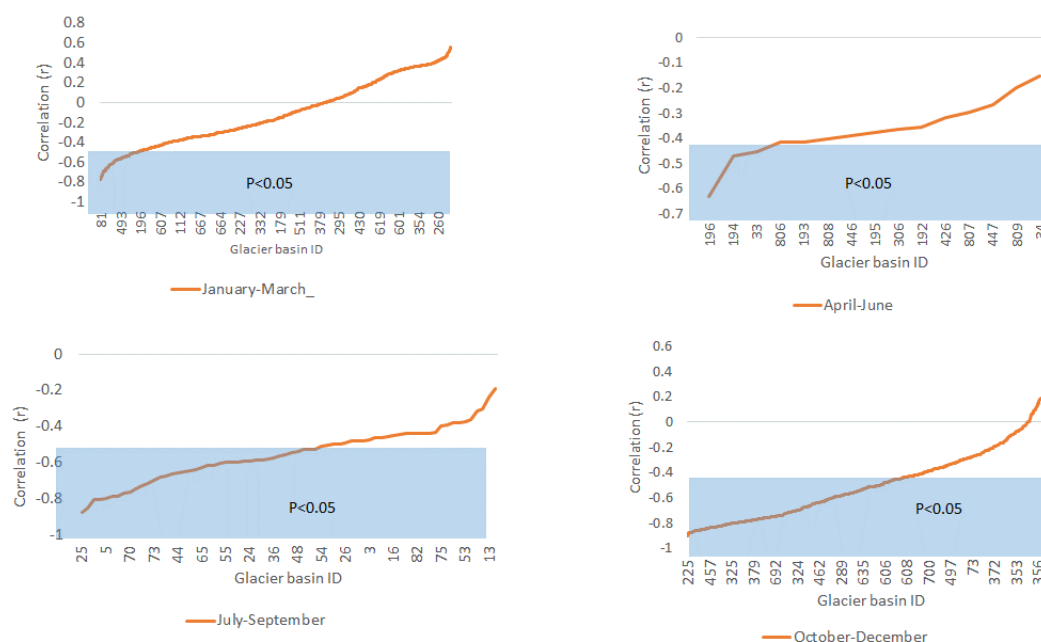
350 **Figure 10. Change in glacier area in glacier basins by directions between 2000 and 2023.**

351 Analysis of snow cover trends indicates that around 63% of glacier basins (n=735) demonstrate negative  
352 correlations from January to March. Among these, glacier basins with a correlation (r) value less than -  
353 0.44 ( $p < 0.05$ ) represent 16.3% of the total (Figure 11, 12, and 13). Basins with moderate negative  
354 correlations, ranging from -0.44 to -0.30, constitute approximately 19% of the overall total. Additionally,  
355 47% of basins show a positive correlation, with 3% being statistically significant and 13% displaying a  
356 moderate correlation. The numerous glacier basins that exhibit negative correlations may suggest a  
357 broader regional trend of declining snow cover over time during winter (January to March). See Figure 8.

358 In the same way, during the months of May, June, and July, all 15 glacier basins that are cloud-free  
359 demonstrate a declining trend in snow cover from 2002 to 2024. Twelve of these basins exhibit a



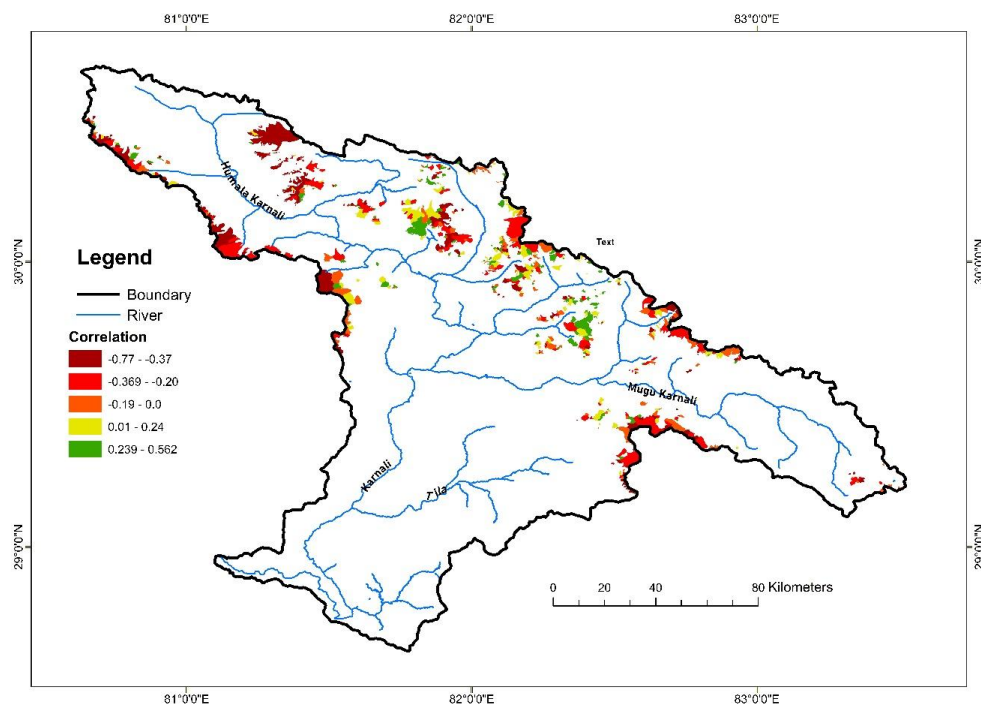
360 moderate negative correlation, meaning  $r$  is less than  $-0.30$ . The trend in snow cover from July to  
361 September also indicates a decline. Approximately 84% of the glacier basins show(n= a statistically  
362 significant negative correlation ( $P < 0.05$ ).



363

364 **Figure 11. The correlation shows the snow cover change between 2002 and 2024 in different glacier**  
365 **basins.**

366 The snow cover trend between July-September and October-December for 22 years also demonstrated a  
367 consistent decline in all glacier basins. Out of 604 basins selected for the analysis, about 60% have shown  
368 a statistically significant negative correlation ( $p < 0.05$ ), and although insignificant, 15 % of glacier basins  
369 showed a moderate negative correlation, i.e.,  $r = -0.47$  to  $-0.30$  (Figure 10). The snow cover in the rest  
370 basins exhibits a poor negative correlation yet indicates a decline in snow cover over the period.



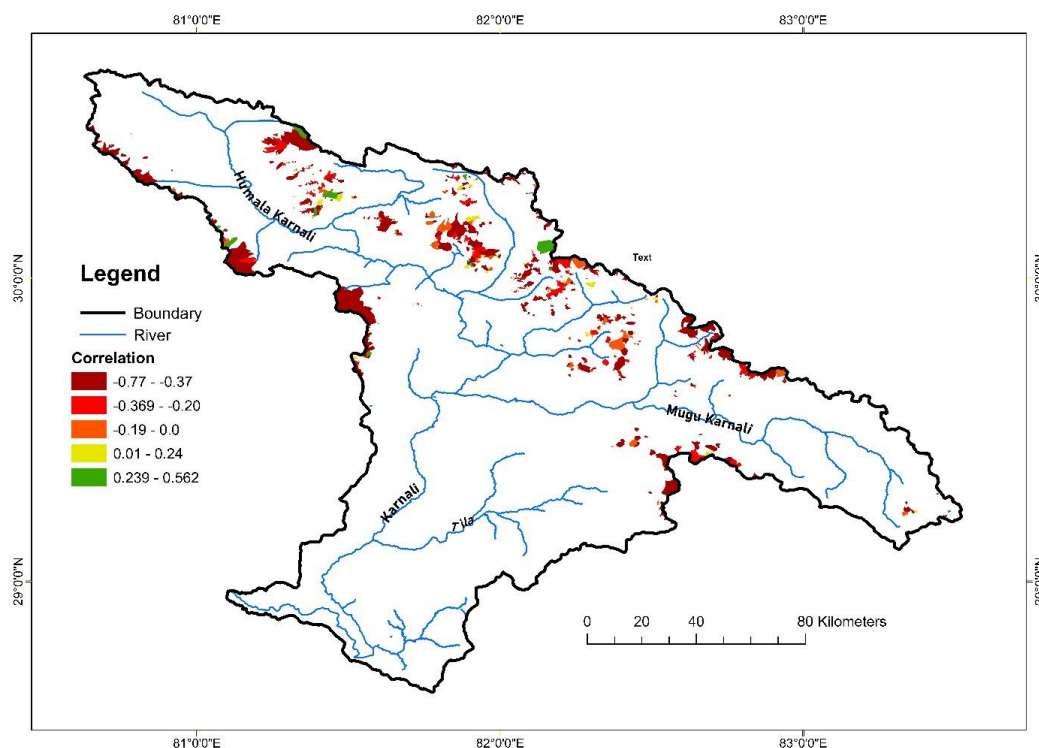
371

372 **Figure 12. Snow cover trend on the Glacier Basins for January-March between 2000-2023 (Landsat**  
373 **5, 7, and 8.**

374

375





376

377 **Figure 13. Snow cover trend on the glacier basins for October-December between 2000-2023**

378 **(Landsat 5, 7, and 8 ).**

#### 379 **4.6. Snowline shift across elevations**

380 The areas covered in snow were derived from the Landsat series 7, 8, and 9 by classifying snow using the  
 381 Normalized Difference Snow Index (NDSI) algorithm to analyze changes in the snowline. This analysis  
 382 was performed on the Google Earth Engine (GEE) platform. Snow pixels were identified with an NDSI  
 383 threshold of  $> 0.4$ . The elevation-wise distribution of snow pixels was then calculated. To determine the  
 384 minimum elevation of the snowline and its shift over the period from 2002 to 2024, three statistical  
 385 thresholds were applied: the 10th, 25th, and 50th percentiles of the snow cover distribution across various  
 386 elevations.



387 The analysis of snowline altitude data from 2002 to 2024 reveals a significant upward trend across all  
388 percentiles (Figure 14). The 10th percentile shows the largest increase, with a Kendall's tau of 0.2662 and  
389 a Sen's slope of approximately 5.16 m/year, indicating that the lower snowline is rising quickly (Table 5).  
390 The 25th percentile presents a moderate yet statistically significant trend, with a Kendall's tau of 0.1938  
391 and a Sen's slope of about 2.91 m/year. In contrast, the 50th percentile displays a gentler trend, with a  
392 Kendall's tau of 0.1483 and a Sen's slope of around 1.54 m/year, which remains statistically significant  
393 ( $p < 0.05$ ). Collectively, these findings suggest that the snowline is progressively moving to higher  
394 elevations, likely reflecting broader climatic changes that are affecting lower elevations more intensively  
395 than the median snowline altitude.

396

397 **Table 5. Statistical Analysis of Snow Line Altitude Trends Using Kendall's Tau and Sen's Slope**

Snow Line Percentile	Kendall's Tau	p-value	Sen's Slope (m/year)	Significance
10th Percentile (SLA_10P)	0.2662	0.00042	5.16	Significant ( $p < 0.001$ )
25th Percentile (SLA_25P)	0.1938	0.01022	2.91	Significant ( $p < 0.05$ )
50th Percentile (SLA_50P)	0.1483	0.04942	1.54	Significant ( $p < 0.05$ )

398

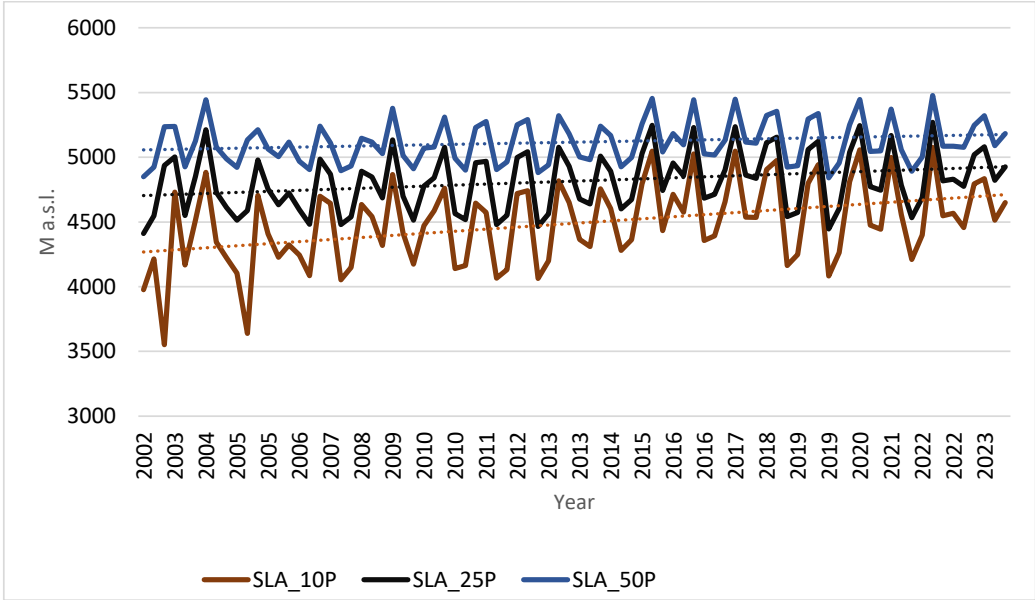


**Figure 14. Snowline shift using snow line of elevation of 10, 25 and 50 percentile**

**5. Discussions**

This study's findings offer important insights into the interactions between snow and ice cover in the Upper Karnali Basin (UKB) and climatic and topographic factors. The results reveal notable trends and fluctuations in snow cover, glacial retreat, and the elevation of the snowline, aligning with the wider patterns of climate change seen in the Himalayan region. We will discuss the key findings below in relation to existing literature and their impact on water resources, ecosystems, and local communities.

The study on the Upper Karnali Basin from 2002 to 2024 reveals significant insights into the relationship between snow cover area (SCA), temperature, and precipitation. The annual average SCA is 872 km<sup>2</sup>, with the highest snow cover occurring from January to March ( $1528 \pm 333$  km<sup>2</sup>) and the lowest from July to September ( $212 \pm 38.3$  km<sup>2</sup>). The findings reveal a gradual decline in snow cover across the Upper Karnali Basin (UKB) from 2002 to 2024, with an average loss of  $\sim 3.99$  km<sup>2</sup>/year.



412 There is a strong to moderate negative correlation between snow cover and temperature across all seasons  
413 ( $r = -0.59$  to  $-0.77$ ,  $p < 0.05$ ), signifying that higher temperatures lead to reduced snow cover. In contrast,  
414 precipitation exhibits a positive correlation with snow cover in winter (January to March and October to  
415 December), although this precipitation does not appear to facilitate snow accumulation. The reduction in  
416 snow cover during winter months (January-March) indicates a potential shift in precipitation patterns,  
417 with more falling as rain instead of snow, resulting in increased snowmelt, aligning with global warming  
418 trends (Wester et al., 2019). During the summer months (April to September), however, precipitation  
419 negatively correlates with snow cover, falling predominantly as rain, thus further enhancing snowmelt.  
420 Particularly, the period from July to September reveals a statistically significant decrease in snow cover  
421 (Sen's Slope =  $-2.87$ ,  $p < 0.05$ ), primarily driven by warmer temperatures and higher rainfall during the  
422 summer monsoon, accelerating snowmelt.

423 The interannual variability in snow cover highlights the sensitivity of snowpack to fluctuating  
424 temperature and precipitation regimes. This variability has significant implications for water availability,  
425 as snowmelt is a critical source of freshwater for downstream communities, agriculture, and hydropower  
426 generation (Immerzeel et al., 2020). The observed decline in snow cover could exacerbate water scarcity  
427 during the dry season, affecting millions of people who rely on snowmelt for irrigation and drinking water  
428 (Pritchard, 2019).

429 Examining snow cover patterns in the UKB sub-basins reveals notable seasonal and spatial differences.  
430 The Humla Karnali sub-basin has the largest average snow cover during January-March, while  
431 downstream areas like Tila and Kawari exhibits

432 The interannual variability in snow cover highlights the sensitivity of snowpack to changing temperature  
433 and precipitation patterns. This variability significantly impacts water availability, as snowmelt serves as  
434 a crucial source of freshwater for downstream communities, agriculture, and hydropower generation  
435 (Immerzeel et al., 2020). The observed reduction in snow cover could worsen water scarcity during the  
436 dry season, affecting millions of people who depend on snowmelt for irrigation and drinking water



437 (Pritchard, 2019). The strong negative correlation in Downstream Karnali ( $r = -0.47$ ,  $p < 0.05$ ) further  
438 highlights the declining trend in snow cover, which could disrupt water availability and ecosystem  
439 services in the region (Wester et al., 2019).

440 The findings emphasize the vulnerability of the UKB to climate change, with rising temperatures and  
441 shifting precipitation patterns leading to reduced snow cover. Adaptive water management strategies are  
442 essential to mitigate the impacts on water resources and local communities.

443 The findings on snow cover dynamics across elevation zones in the Upper Karnali Basin reveal  
444 significant elevation-dependent patterns, driven by temperature fluctuations and global warming. At  
445 lower elevations ( $\leq 2000$  m a.s.l.), snow cover exhibits a weak positive correlation (0.12–0.43), suggesting  
446 a marginal increase, likely due to localized precipitation variability. However, this is accompanied by  
447 high interannual variability (CoV  $\sim 41$ –43%), indicating sensitivity to fluctuating temperature and  
448 precipitation regimes (Pepin et al., 2015). This variability underscores the vulnerability of lower  
449 elevations to climate change, where even minor temperature increases can significantly impact snow  
450 accumulation and melt.

451 The transition from weak negative correlations above 2300 m above sea level (m a.s.l.) to the strongest  
452 negative correlation at 6100–6200 m a.s.l. ( $r = -0.56$ ) corresponds with comprehensive evidence of  
453 elevation-dependent warming (EDW) identified in recent studies. It has been globally observed that  
454 higher altitudes experience accelerated warming, leading to reduced snow accumulation and increased  
455 melt rates (Elevation-dependent warming in mountain regions of the world, 2015; Krishnan et al., 2019;  
456 Pepin et al., 2022; Shen et al., 2021; Naegeli et al., 2019) The sharp rise in mean snow cover above 5000  
457 m a.s.l. coincides with permanent snow and glacier zones, but the decline in inter-annual variability  
458 (CoV) suggests a consistent reduction in snow cover, particularly at mid-to-high elevations (3000–5000  
459 m a.s.l.).



460 The nonlinear relationship between elevation and snow cover variability (CoV) proves particularly  
461 insightful. Below 3100 m a.s.l., CoV reaches 41–43%, reflecting transitional zones where slight  
462 temperature fluctuations determine precipitation phase (rain vs. snow). Above 3,100 m a.s.l., CoV drops  
463 to 25–30% as conditions remain persistently below freezing, but the dominant driver shifts to insolation  
464 and temperature-modulated melt rates. This aligns with Ren et al.'s (2023) findings on Tibetan Plateau  
465 glaciers, where albedo feedbacks dominate mass balance above 5000 m a.s.l.

466 The strong negative correlation between land surface temperature and snow cover ( $\text{Tau} = -0.43$  to  $-0.79$ )  
467 further highlights the impact of rising temperatures on snowpack. The most severe declines occur  
468 between 3000–5000 m a.s.l., where warming accelerates snowmelt and glacier retreat, threatening water  
469 availability for river flows, agriculture, and hydropower (Immerzeel et al., 2020). This elevation-  
470 dependent warming exacerbates glacier mass loss, leading to a negative mass balance and reduced  
471 freshwater storage, which has profound implications for downstream communities reliant on meltwater  
472 (Bolch et al., 2012).

473 Snow cover trends in glacier basins within the Upper Karnali Basin reveals significant declines in both  
474 glacier area and snow cover from 2000 to 2023. The mean glacier area decreased from 119.046 hectares  
475 in 2000 to 100.472 hectares in 2023, reflecting an average loss of 18.574 hectares per basin. This  
476 widespread glacier retreat is consistent across all basin orientations, with the most significant losses  
477 observed in north-facing basins (N, NW, NE), totaling -6,126.9 hectares. The reduction in glacier area is  
478 attributed to rising temperatures and decreased snowfall, which disrupt the glacier mass balance, leading  
479 to accelerated melting and negative mass balance (Pepin et al., 2022; Ye and Tian, 2022; Pei Ren et al.,  
480 2024). The decline in permanent snow cover further exacerbates these effects, threatening glacier  
481 persistence and altering water availability.

482 Snow cover trends in glacier basins also show a consistent decline, particularly during winter (January-  
483 March) and post-monsoon (October- December) seasons. Approximately 63% of glacier basins exhibit  
484 negative correlations in snow cover from January to March, with 16.3% showing statistically significant



485 declines ( $r < -0.44$ ,  $p < 0.05$ ). Similarly, 84% of glacier basins demonstrate significant negative  
486 correlations in snow cover from July to September, indicating a substantial seasonal decline. The  
487 reduction in snow cover is linked to rising temperatures, which increase snowmelt rates and reduce  
488 albedo, further accelerating glacier retreat (Dowson et al., 2020). These trends highlight the vulnerability  
489 of glacier basins to climate change, with significant implications for water security and regional  
490 hydrology.

491 One of the most alarming findings is the steady upward migration of the snowline, as revealed by the  
492 snow elevation percentile analysis. The 10th percentile snowline has shifted upward by ~5.6 meters per  
493 year, while the 25th and 50th percentiles show a more moderate but significant rise (~2.91 and 1.54  
494 meters per year, respectively). This indicates a systematic retreat of seasonal snow cover to higher  
495 elevations, reducing the snow accumulation potential for glacier mass balance maintenance.

#### 496 **Feedback mechanisms and future projections**

497 The temperature–snow cover correlation ( $\tau = -0.43$  to  $-0.79$  across elevations) establishes a reinforcing  
498 feedback loop: 1. Warming reduces snow cover, lowering surface albedo, 2. Absorbed solar radiation  
499 increases local temperatures by 0.8–1.2°C (estimated from Sen’s slope), and enhanced melting further  
500 reduces albedo, accelerating the cycle.

501 At current warming rates (0.0643°C/year above 5,000 m a.s.l.), the UKB could lose 70–80% of its glacier  
502 area by 2050, reflecting Ye and Tian’s (2022) projections for the central Himalayas. This would  
503 transform the basin’s hydrology from nival (snowmelt-dominated) to pluvial (rain-dominated), increasing  
504 flood risks during monsoons and drought susceptibility in dry seasons.

505 The findings highlight the continuing effects of climate change on glacier-fed regions. Increasing  
506 temperatures and changing precipitation patterns are causing reductions in glacier area and snow cover,  
507 which has significant implications for water resources, ecosystems, and local communities dependent on  
508 glacier meltwater.



509

## 510 **Conclusions**

511 The study of snow and glacier cover dynamics in the Upper Karnali Basin from 2002 to 2024 reveals a  
512 persistent decline in snow cover, glacier area, and snowline elevation, driven by rising temperatures and  
513 altered precipitation patterns.

514 The annual snow-covered area (SCA) has decreased by approximately 3.99 km<sup>2</sup> per year, with the most  
515 significant reductions observed during the July-September monsoon period. The decline in snow cover is  
516 statistically correlated with increasing temperatures, demonstrating the impact of climate change on  
517 seasonal snow accumulation and melt cycles. The winter snow cover variability suggests changes in  
518 snowfall patterns rather than a uniform decrease.

519 Notable seasonal and spatial differences in snow cover patterns are observed in the Sub-basins of UKB  
520 for two seasons, January-March and October-December. The upstream sub-basins experience less  
521 inconsistent snowfall than the downstream basins. During October-December, snowfall is inconsistent in  
522 all basins, but more inconsistent in particularly China Karnali, Tila and Downstream Karnali.

523 Elevation-dependent trend analysis confirms that snow cover at lower elevations (<2000 m a.s.l.) exhibits  
524 high interannual variability, while higher elevations (>3000 m a.s.l.) show a significant long-term decline.  
525 The strongest reductions occur between 3000–5000 m a.s.l., where warming accelerates snowmelt and  
526 glacier retreat. The observed negative correlation between snow cover and rising temperatures confirms  
527 the climate-driven reduction in snowpack, exacerbating the risk of water shortages.

528 The study of glacier basins shows widespread retreat, with the mean glacier area declining from 119.046  
529 hectares in 2000 to 100.472 hectares in 2023. Glacier retreat is most pronounced in north-facing basins  
530 (N, NW, NE), where melting exceeds accumulation. The continuous decline in snow cover across glacier  
531 basins indicates an ongoing negative mass balance, threatening long-term glacier persistence.





532 Additionally, the snow line is gradually shifting upward, with the 10th, 25th, and 50th percentiles rising  
533 by approximately 5.16, 2.91, and 1.54 meters per year, respectively, indicating a consistent loss of  
534 seasonal snow accumulation.

535 Given the current warming trends ( $\sim 0.0643^{\circ}\text{C}/\text{year}$  above 5000 m a.s.l.), the UKB could experience a 70-  
536 80% reduction in glacier area by 2050. This would transform the hydrology from snowmelt-dominated  
537 (nival) to rainfall-dominated (pluvial), increasing the frequency of extreme weather events and altering  
538 regional water security dynamics. The findings emphasize the need for proactive water resource  
539 management, improved climate resilience strategies, and continuous monitoring of cryospheric changes to  
540 mitigate future risks. Policymakers must prioritize adaptation measures, such as improved water storage  
541 infrastructure and sustainable land-use practices, to ensure long-term water security in the Upper Karnali  
542 Basin and beyond.

#### 543 **Author contributions**

544 MG conceptualized the research, designed the methodology, conducted fieldwork, analyzed the data, and  
545 drafted the manuscript. DS. and RC assisted in proposal writing, research design, fieldwork, and data  
546 analysis. AT, TPPS, KPS, SBG, and SD contributed to procuring remote sensing and climate data. PB  
547 and SK were responsible for procuring and updating MODIS data. WY reviewed the manuscript and  
548 provided feedback to enhance its quality. NT and JK assisted in GIS analysis. All authors contributed to  
549 revising the manuscript and provided input before submission.

#### 550 **Competing Interests**

551 The authors declare that they have no conflict of interest.

552



553 **Acknowledgments**

554 We express our gratitude to the Director of Tribhuvan University's Research Coordination and  
555 Development Council (RCDC) for supporting the project titled "State and Dynamics of the Cryosphere of  
556 the Upper Karnali Basin, Associated Hazards and Implications for Water Resources and Livelihood"  
557 (Project Code TU-NPAR-077/78-ERG-15). This paper is a product of that project. We appreciate the  
558 Evaluation and Monitoring Committee of RCDC for their insightful feedback and suggestions, which  
559 greatly enhanced the manuscript. We also thank the University Grants Commission for providing research  
560 funding. Authors would also like to sincerely acknowledge the Sichuan Science and Technology  
561 Program (2024YFHZ0248) for partial support. We also acknowledge the contributions of Google Earth  
562 Engine, ERA5, ESRI, and other open-access resources for providing satellite imagery and data.

563 **Financial support**

564 This research was funded by the University Grants Commission (UGC), Kathmandu, through Tribhuvan  
565 University's Research Coordination and Development Council (RCDC) under the National Policy Area  
566 Research program. The Sichuan Science and Technology Program (2024YFHZ0248) also provided  
567 partial funding for this research.

568 **References**

- 569 Anup, K. (2017). Climate change and its impact on tourism in Nepal. *Journal of Tourism and Hospitality*  
570 *Education*, 7, 25-43.
- 571 Bajracharya, S. R., Bajracharya, O. R., Baidya, S., Maharjan, S. B., & Shrestha, F. 2014 (2014) 'Climate  
572 change impact on glaciers in the Langtang and Imja sub-basins of Nepal from late 70s to 2010' *AGU Fall*  
573 *Meeting Abstracts*. pp. C31B-0278.
- 574 Bajracharya, S. R., Mool, P. K., & Shrestha, B. R. (2008). Global climate change and melting of Himalayan  
575 glaciers. *Melting glaciers and rising sea levels: Impacts and implications*, 28-46.



- 576 Bishop, M. P., Olsenholler, J. A., Shroder, J. F., Barry, R. G., Raup, B. H., Bush, A. B., et al. (2004). Global  
577 Land Ice Measurements from Space (GLIMS): remote sensing and GIS investigations of the Earth's  
578 cryosphere. *Geocarto International*, 19(2), 57-84.
- 579 Bolch, T. (2007). Climate change and glacier retreat in northern Tien Shan (Kazakhstan/Kyrgyzstan) using  
580 remote sensing data. *Global and Planetary Change*, 56(1-2), 1-12.
- 581 Bolch, T., Kulkarni, A., Kääb, A., Huggel, C., Paul, F., Cogley, J. G., et al. (2012). The state and fate of  
582 Himalayan glaciers. *Science*, 336(6079), 310-314.
- 583 Bookhagen, B., & Burbank, D. W. (2010). Toward a complete Himalayan hydrological budget:  
584 Spatiotemporal distribution of snowmelt and rainfall and their impact on river discharge. *Journal of*  
585 *Geophysical Research: Earth Surface*, 115(F3).
- 586 Dowson, A. J., Sirguey, P., & Cullen, N. J. (2020). Variability in glacier albedo and links to annual mass  
587 balance for the gardens of Eden and Allah, Southern Alps, New Zealand. *The Cryosphere*, 14(10), 3425-  
588 3448.
- 589 Elevation-dependent warming in mountain regions of the world (2015). *Nature climate change*, 5(5),  
590 424-430.
- 591 Elsasser, H., & Bürki, R. (2002). Climate change as a threat to tourism in the Alps. *Climate research*,  
592 20(3), 253-257.
- 593 Forster, P., Storelvmo, T., & Alterskjær, K. (2021) 'IPCC sixth assessment report (AR6) working group 1:  
594 the physical science basis, chap. 7'. University Press, UK, [https://www.ipcc.](https://www.ipcc.ch/report/ar6/wg1/downloads)  
595 [ch/report/ar6/wg1/downloads](https://www.ipcc.ch/report/ar6/wg1/downloads) (last ....
- 596 Gorelick, N., Hancher, M., Dixon, M., Ilyushchenko, S., Thau, D., & Moore, R. (2017). Google Earth  
597 Engine: Planetary-scale geospatial analysis for everyone. *Remote sensing of Environment*, 202, 18-27.



- 598 Gurung, D. R., Maharjan, S. B., Shrestha, A. B., Shrestha, M. S., Bajracharya, S. R., & Murthy, M. (2017).  
599 Climate and topographic controls on snow cover dynamics in the Hindu Kush Himalaya. *Int. J. Climatol*,  
600 37(10), 3873-3882.
- 601 Hall, D. K., Riggs, G. A., Salomonson, V. V., DiGirolamo, N. E., & Bayr, K. J. (2002). MODIS snow-cover  
602 products. *Remote sensing of Environment*, 83(1-2), 181-194.
- 603 Heid, T., & Kääb, A. (2012). Repeat optical satellite images reveal widespread and long term decrease in  
604 land-terminating glacier speeds. *The Cryosphere*, 6(2), 467-478.
- 605 Hersbach, H., Bell, B., Berrisford, P., Hirahara, S., Horányi, A., Muñoz-Sabater, J., et al. (2020). The ERA5  
606 global reanalysis. *Quarterly journal of the royal meteorological society*, 146(730), 1999-2049.
- 607 Immerzeel, W. W., Lutz, A. F., Andrade, M., Bahl, A., Biemans, H., Bolch, T., et al. (2020). Importance and  
608 vulnerability of the world's water towers. *Nature*, 577(7790), 364-369.
- 609 Kääb, A., Berthier, E., Nuth, C., Gardelle, J., & Arnaud, Y. (2012). Contrasting patterns of early twenty-  
610 first-century glacier mass change in the Himalayas. *Nature*, 488(7412), 495-498.
- 611 Kääb, A., Huggel, C., Fischer, L., Guex, S., Paul, F., Roer, I., et al. (2005). Remote sensing of glacier-and  
612 permafrost-related hazards in high mountains: an overview. *Natural Hazards and Earth System Sciences*,  
613 5(4), 527-554.
- 614 Krishnan, R., Shrestha, A. B., Ren, G., Rajbhandari, R., Saeed, S., Sanjay, J., et al. (2019). Unravelling  
615 climate change in the Hindu Kush Himalaya: rapid warming in the mountains and increasing extremes.  
616 *The Hindu Kush Himalaya assessment: Mountains, climate change, sustainability and people*, 57-97.
- 617 Kulkarni, A. V., Shirsat, T. S., Kulkarni, A., Negi, H., Bahuguna, I., & Thamban, M. (2021). State of  
618 Himalayan cryosphere and implications for water security. *Water Security*, 14, 100101.



- 619 Mimura, N. (2013). Sea-level rise caused by climate change and its implications for society. *Proceedings*  
620 *of the Japan Academy, Series B*, 89(7), 281-301.
- 621 Mishra, B., Babel, M. S., & Tripathi, N. K. (2014). Analysis of climatic variability and snow cover in the  
622 Kaligandaki River Basin, Himalaya, Nepal. *Theoretical and applied climatology*, 116, 681-694.
- 623 Mool, P. K., Bajracharya, S. R., & Joshi, S. P. (2001). Inventory of glaciers, glacial lakes and glacial lake  
624 outburst floods. Monitoring and early warning systems in the Hindu Kush-Himalayan Region: Nepal.
- 625 Muhammad, S., & Thapa, A. (2020). An improved Terra–Aqua MODIS snow cover and Randolph Glacier  
626 Inventory 6.0 combined product (MOYDGL06\*) for high-mountain Asia between 2002 and 2018. *Earth*  
627 *System Science Data*, 12(1), 345-356.
- 628 Naegeli, K., Huss, M., & Hoelzle, M. (2019). Change detection of bare-ice albedo in the Swiss Alps. *The*  
629 *Cryosphere*, 13(1), 397-412.
- 630 NOAA (2013). Sea Levels Online. . NOAA. <https://tidesandcurrents.noaa.gov/sltrends/sltrends.html>.  
631 Accessed.
- 632 Nyaupane, G. P., & Chhetri, N. (2009). Vulnerability to climate change of nature-based tourism in the  
633 Nepalese Himalayas. *Tourism Geographies*, 11(1), 95-119.
- 634 Pendergrass, A. G. (2020). Changing degree of convective organization as a mechanism for dynamic  
635 changes in extreme precipitation. *Current Climate Change Reports*, 6, 47-54.
- 636 Pepin, N. C., Arnone, E., Gobiet, A., Haslinger, K., Kotlarski, S., Notarnicola, C., et al. (2022). Climate  
637 changes and their elevational patterns in the mountains of the world. *Reviews of geophysics*, 60(1),  
638 e2020RG000730.
- 639 Pfeffer, W. T., Arendt, A. A., Bliss, A., Bolch, T., Cogley, J. G., Gardner, A. S., et al. (2014). The Randolph  
640 Glacier Inventory: a globally complete inventory of glaciers. *Journal of glaciology*, 60(221), 537-552.



- 641 Pritchard, H. D. (2019). Asia's shrinking glaciers protect large populations from drought stress. *Nature*,  
642 569(7758), 649-654.
- 643 Ren, P., Pan, X., Liu, T., Huang, Y., Chen, X., Wang, X., et al. (2024). Glacier changes from 1990 to 2022 in  
644 the Aksu River Basin, western Tien Shan. *Remote Sensing*, 16(10), 1751.
- 645 Ren, S., Jia, L., Menenti, M., & Zhang, J. (2023). Changes in glacier albedo and the driving factors in the  
646 Western Nyainqentanglha Mountains from 2001 to 2020. *Journal of Glaciology*, 69(277), 1500-1514.
- 647 Shen, L., Zhang, Y., Ullah, S., Pepin, N., & Ma, Q. (2021). Changes in snow depth under elevation-  
648 dependent warming over the Tibetan Plateau. *Atmospheric Science Letters*, 22(9), e1041.
- 649 Shrestha, A. B., & Aryal, R. (2011). Climate change in Nepal and its impact on Himalayan glaciers.  
650 *Regional environmental change*, 11, 65-77.
- 651 Shrestha, M., Wang, L., Koike, T., Xue, Y., & Hirabayashi, Y. (2012). Modeling the spatial distribution of  
652 snow cover in the Dudhkoshi region of the Nepal Himalayas. *Journal of Hydrometeorology*, 13(1), 204-  
653 222.
- 654 Wester, P., Mishra, A., Mukherji, A., & Shrestha, A. B. (2019). The Hindu Kush Himalaya assessment:  
655 mountains, climate change, sustainability and people. Springer Nature.
- 656 Xu, J., Grumbine, R. E., Shrestha, A., Eriksson, M., Yang, X., Wang, Y., et al. (2009). The melting  
657 Himalayas: cascading effects of climate change on water, biodiversity, and livelihoods. *Conservation*  
658 *Biology*, 23(3), 520-530.
- 659 Ye, Y., & Tian, Y. (2022). Interpreting changes in albedo and mass balance at White Glacier, Canadian  
660 Arctic Archipelago. *The International Archives of the Photogrammetry, Remote Sensing and Spatial*  
661 *Information Sciences*, 43, 793-798.



- 662 Zemp, M. (2006) *Glaciers and climate change: spatio-temporal analysis of glacier fluctuations in the*  
663 *European Alps after 1850*. University of Zurich
- 664 NASA LP DAAC. (2023). *MODIS/Aqua Land Surface Temperature and Emissivity 8-Day L3 Global 1*  
665 *km SIN Grid, Version 6.1* [Data set]. NASA Land Processes Distributed Active Archive Center (LP  
666 DAAC). Accessed via AppEEARS on 2025-02-15. Available at:  
667 <https://doi.org/10.5067/MODIS/MYD11A2.061>
- 668 ECMWF. (2023). *ERA5: Fifth generation of ECMWF atmospheric reanalyses of the global climate*.  
669 Copernicus Climate Change Service (C3S). Retrieved from <https://cds.climate.copernicus.eu/>